

# The Modern Student Laboratory

## Physical Chemistry

### Fluorescence Anisotropy Measurements in Undergraduate Teaching

Stephen W. Bigger

Department of Environmental Management, Victoria University of Technology, St. Albans Campus, St. Albans, 3021, Australia

Robert A. Craig and Kenneth P. Ghiggino

School of Chemistry, The University of Melbourne, Parkville, 3052, Australia

John Scheirs

Department of Mechanical and Manufacturing Engineering, The University of Melbourne, Parkville, 3052, Australia

Fluorescence measurements are widely used as a means of obtaining information about molecular energy levels and molecular structure (1). A most useful application of steady-state fluorimetry is the technique of fluorescence anisotropy (or depolarization), which can be used to give information about the rotational dynamics of molecules in solution. The exploratory work in this field was carried out by Perrin in the early 1920's, and this gave rise to the seminal papers (2, 3) on this subject.

Steady-state and time-resolved fluorescence anisotropy measurements have been used successfully and extensively in the study of the rotational motion of proteins (4-9) and synthetic polymers (10-21) as well as in the probing of the structures of bilayers and lipids (22-24).

In this article, we

- discuss how the Perrin equation can be applied to fluorescence data
- describe a simple experiment that demonstrates to students an application of fluorescence anisotropy measurements
- describe a simplified approach to understanding the nature of the limiting fluorescence anisotropy phenomenon

#### Fluorescence Polarization Apparatus

##### Design of the Polarimeter

Fluorescence anisotropy experiments can be carried out using a fluorescence polarization apparatus. The polarimeter constructed and used in our laboratory is illustrated schematically in Figure 1. It is based on a design described by Bashford and coworkers (25).

The light from a 150-W xenon arc lamp (Osram XBO-150 W/1, driven by a Cathodeon power supply) is directed onto the entrance slit of a high-throughput monochromator (Bausch and Lomb 33-86-07; 1200 grooves/mm) set to the appropriate excitation wavelength (in our case 386 nm). The excitation beam emerging from the monochromator is focussed through a lens and passed through a polarizing filter (Polacoat 105-UV) before it reaches the sample.

The sample is contained in a standard 1-cm path length fluorescence cell mounted in a temperature-controlled holder. The fluorescence emission is detected at right angles to the excitation beam by two photomultiplier tubes (EMI type 9804B) mounted on either side of the sample. The emission is isolated from scattered excitation light using an appropriate cut-off filter (Schott GG 400).

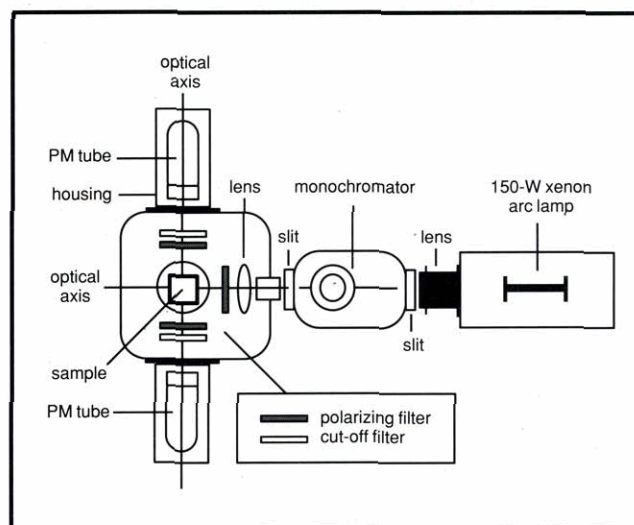


Figure 1. Schematic diagram of fluorescence polarimeter.

##### Excitation and Emission

The polarizing filter in the excitation beam causes the sample to be excited with plane-polarized light. The only molecules excited will be those with a component of their absorption transition moment parallel to the electric vector of the excitation beam. If the transition moments for absorption and fluorescence are the same (which is true in many cases), and the molecule emits but does not rotate, then the fluorescence will be depolarized to some extent due to the random distribution of molecular orientations (1). However, if molecular rotation occurs during the excited-state lifetime, then additional depolarization of the fluorescence will result.

The photomultiplier tubes are used to quantitatively determine the fluorescence anisotropy (or "depolarization") by measuring the intensity of fluorescence emission polarized parallel ( $I_{\parallel}$ ) and perpendicular ( $I_{\perp}$ ) to the direction of polarization of the excitation beam (1, 26, 27). This is achieved by placing a suitably oriented polarizing filter (Polacoat 105-UV) in front of each of the photomultiplier tubes.

(Continued on page A236)



## The Perrin Equation

It is usual to define  $P$ , the degree of polarization, as

$$P = \frac{I_{\parallel} - I_{\perp}}{I_{\parallel} + I_{\perp}} \quad (1)$$

The relationship between  $P$  and  $\alpha$ , the angle between the absorption and the emission transition moments of the fluorophore ( $I$ ), is given by

$$P = \frac{3\cos^2 \alpha - 1}{\cos^2 \alpha + 3} \quad (2)$$

The fluorescence emission anisotropy  $A$  is defined (28, 29) as follows.

$$A = \frac{I_{\parallel} - I_{\perp}}{I_{\parallel} + 2I_{\perp}} \quad (3)$$

### Correction for Variations in the Transmission

However, if fluorescence depolarization experiments are carried out using a conventional fluorimeter or a simplified fluorimeter constructed for undergraduate teaching (30), then a correction must be made to allow for systematic variations in the transmission of  $I_{\parallel}$  and  $I_{\perp}$  through the detection system (27). In these cases, the anisotropy is calculated using eq 4.

$$A = \frac{I_{VV} - GI_{VH}}{I_{VV} + 2GI_{VH}} \quad (4)$$

where  $I_{VV}$  and  $I_{VH}$  are the fluorescence intensities determined using vertically polarized excitation light, while monitoring vertically polarized and horizontally polarized emission, respectively.

$$G = \frac{I_{HV}}{I_{HH}}$$

where  $G$  is the instrumental correction factor; and  $I_{HV}$  and  $I_{HH}$  are the vertically and horizontally polarized fluorescence intensities using horizontally polarized excitation light.

The Perrin equation (2, 3) can be written as

$$\frac{1}{A} = \frac{1}{A_0} \left( 1 + \frac{3\tau_f}{\tau_{\text{rot}}} \right) \quad (5)$$

where  $A_0$  is the limiting emission anisotropy (i.e., the anisotropy in the absence of fluorophore rotation); and  $\tau_f$  and  $\tau_{\text{rot}}$  are the fluorescence lifetime and the rotational correlation time of the fluorophore, respectively. The rotational correlation time is the time taken for the initial anisotropy to fall to  $1/e$  of its original value due to molecular rotation.

### Rotational Mobility of the Emitter

Experimental determination of the anisotropy can lead to an estimation of  $\tau_{\text{rot}}$ , thereby providing information on the rotational mobility of the emitter. For a protein with an attached fluorophore, the value of  $\tau_{\text{rot}}$  can reflect the ease of rotation either for the macromolecule as a whole or for an internal rotation of its parts.

For example, the lower experimental value of  $\tau_{\text{rot}}$  determined for immunoglobulin G compared to the value expected for rotation of the whole protein has been interpreted as evidence for internal flexibility in the macromolecule (31). In the case of concanavalin A, changes in  $\tau_{\text{rot}}$  with pH are assigned to changes in the conformation of the

protein (32). With enzymes and other biological macromolecules, this conformational behavior is believed to affect their specific activity and function. These factors have been discussed by Wahl (33).

### Hydrodynamic Molar Volume of a Globular Protein

An experiment that demonstrates an application of the Perrin equation is one in which a fluorescent probe (8-anilino-1-naphthalene sulfonic acid, ANS,  $\lambda_{\text{max}}(\text{fl}) = 460 \text{ nm}$ ) is attached to a protein molecule (bovine serum albumin (BSA), Sigma) in a buffered solution of pH = 7.2. Then the molar volume of the resulting dye-polymer conjugate is determined.

To do this, the rotational correlation time ( $\tau_{\text{rot}}$ ) in eq 5 can be obtained from the Stokes-Einstein equation (34).

$$\tau_{\text{rot}} = \frac{V\eta}{RT} \quad (6)$$

where  $V$  is the molar volume of the dye-polymer conjugate assuming its shape to be spherical;  $\eta$  is the viscosity of the solution;  $R$  is the ideal gas constant; and  $T$  is the absolute temperature.

The volume of one molecule of the conjugate is equal to

$$\frac{V}{N_A}$$

where  $N_A$  is the Avogadro constant.

From eqs 5 and 6 the Perrin equation can be written as

$$\frac{1}{A} = \frac{1}{A_0} \left( 1 + \frac{3\tau_f RT}{V\eta} \right) \quad (7)$$

If a dilute aqueous solution of the protein is used (0.40 g  $\text{L}^{-1}$  BSA in the presence of  $8 \times 10^{-6} \text{ M}$  ANS), then the viscosity of the solution is approximately equal to the viscosity of water. Although the ANS probe is nonfluorescent in water, it becomes highly fluorescent when it is non-covalently bound to the BSA on mixing. Thus, any ANS that is unbound to the protein should not interfere with the anisotropy measurements.

Students should be told that there are possible pitfalls associated with the adsorption of dyes, as compared with covalent labelling. For example, the presence of multiple binding sites in BSA (35, 36) could produce erroneous anisotropic data if the concentration of ANS used is too high. Furthermore, most proteins display weaker binding and less fluorescence enhancement with ANS than does BSA (37).

Using eq 3 (or eq 4) values of  $1/A$  can be calculated from experimental measurements at different temperatures from, for example, 25 to 60 °C, and plotted against  $T/\eta$  (see Fig. 2). The viscosity of water at different temperatures is obtained from tabulated data (38). The intercept of the plot is equal to  $1/A_0$ , and the gradient is equal to  $3\tau_f R/(A_0 V)$ . Thus, the value of  $V$  can be determined given that  $\tau_f(\text{ANS-BSA}) = 15.6 \text{ ns}$ , making the valid assumption that the value of  $\tau_f$  remains essentially constant over the temperature range of the measurements.<sup>1</sup>

The molar volume of BSA calculated from the data presented in Figure 2 is  $0.132 \text{ m}^3 \text{ mol}^{-1}$ , which compares favorably

<sup>1</sup>The value of  $\tau_f(\text{ANS-BSA})$  was determined over the temperature range of 15 to 60 °C in our laboratory using a laser-based, time-correlated, single-photon counting system. It was found to remain constant to within about 8%.

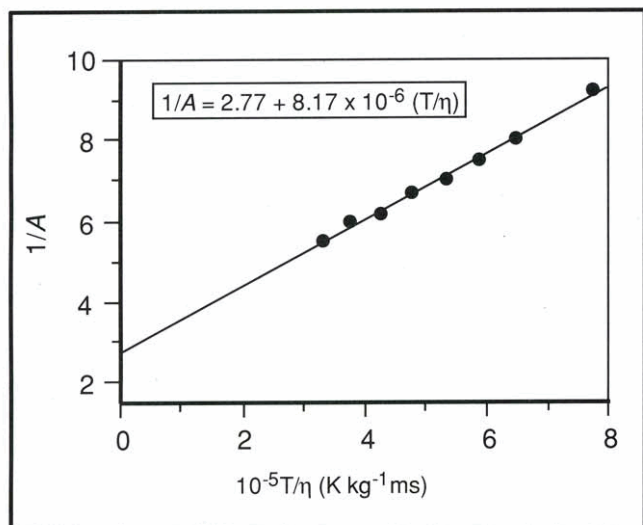


Figure 2. Plot of  $1/A$  versus  $T/\eta$  for  $0.40 \text{ g L}^{-1}$  bovine serum albumin labelled with  $8 \times 10^{-6} \text{ M}$  ANS (excitation wavelength:  $386 \text{ nm}$ ; fluorescence emission monitored at  $460 \text{ nm}$ ).

ably with the value of about  $0.104 \text{ m}^3 \text{ mol}^{-1}$  determined from X-ray scattering experiments (39). The molar volume calculated from the fluorescence measurements is expected to be larger because it is a hydrodynamic value: It includes the sheath of water molecules that surround the protein molecule and move with it in solution. On the other

hand, X-ray scattering experiments on crystalline polymers reveal the molecular volume in the solid state.

An alternative approach to the experimental procedure is to keep the temperature constant (e.g.,  $25^\circ \text{C}$ ) and vary the solution viscosity by adding different quantities of glycerol. However, this is a more time-consuming method because the viscosity of each test solution must be determined by an appropriate method (e.g., capillary viscometry).

#### Limiting Emission Anisotropy

It has been our experience that students often have difficulty understanding why  $A_o < 1$  as a result of the random orientation of transition moments in a molecular ensemble. The original work by Perrin (2, 3) is rather inaccessible and of limited help because it is mathematically advanced, especially in its use of spherical harmonics. The following, comparatively simpler, approach has proven to be a successful method of teaching the phenomenon of the limiting emission anisotropy.

Consider the hypothetical case in which there is no molecular rotation during the excited state lifetime of the fluorophore. If the angle between the absorption and emission transition moments is zero, then  $P = 0.5$  ( $\alpha = 0$ , in eq 2). Thus,  $I_{\parallel} = 3I_{\perp}$  (from eq 1). The limiting emission anisotropy  $A_o$  is equal to 0.4 in this case (see eq 3).

(Continued on next page)



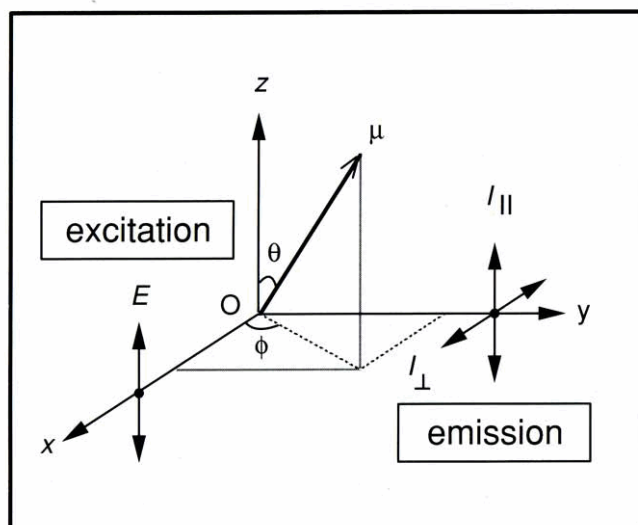


Figure 3. Vector diagram showing a schematic representation of the fluorescence depolarization phenomenon.

Figure 3 is a vector diagram that applies to this situation. The sample is located at the origin. The excitation beam  $E$  is directed along  $Ox$  and is polarized in the  $z$  direction. The transition moment in the sample molecule is  $\mu$  and has orientation  $(\theta, \phi)$ . The intensity of fluorescence emission (along  $Oy$ ) polarized parallel to the  $z$  axis is  $I_{||}$  and is proportional to the square of the component of  $\mu$  in the  $z$  direction.

$$I_{||} \equiv (\mu_z)^2 = |\mu|^2 \cos^2 \theta \quad (8)$$

where the symbol  $\equiv$  means "is equivalent to".

Similarly, the intensity of fluorescence emission polarized parallel to the  $x$  axis is  $I_{\perp}$  and is given by

$$I_{\perp} \equiv (\mu_x)^2 = |\mu|^2 (\sin^2 \theta)(\cos^2 \phi) \quad (9)$$

Now  $|\mu|$  itself will be proportional to the component of  $E$  along  $\mu$ . However, for simplicity the magnitudes of both  $E$  and  $\mu$  can be taken as unity. Hence,

$$|\mu| \equiv \cos \theta$$

Thus,

$$I_{||} \equiv \cos^4 \theta \quad \text{and} \quad I_{\perp} \equiv (\cos^2 \theta)(\sin^2 \theta)(\cos^2 \phi)$$

Averaging over all orientations  $(\theta, \phi)$  of the transition moment and recalling that the integration element is  $\sin \theta d\theta d\phi$ , we can apply eqs 10 and 11.

$$\langle I_{||} \rangle = \frac{\int_0^{2\pi} \int_0^{\pi} (\cos^4 \theta)(\sin \theta) d\theta d\phi}{\int_0^{2\pi} \int_0^{\pi} \sin \theta d\theta d\phi} \quad (10)$$

$$\langle I_{\perp} \rangle = \frac{\int_0^{2\pi} \int_0^{\pi} \cos^2 \phi d\phi \int_0^{\pi} (\cos^2 \theta)(\sin^3 \theta) d\theta}{\int_0^{2\pi} \int_0^{\pi} \sin \theta d\theta d\phi} \quad (11)$$

```
p=3.14159
d=.1
FOR theta=0 TO p STEP d
  FOR phi=0 TO 2*p STEP d
    az=COS(theta)^4*SIN(theta)
    ax=COS(phi)^2*COS(theta)^2*SIN(theta)^3
    sumz=sumz+az*d*d
    sumx=sumx+ax*d*d
  NEXT phi
PRINT USING "Theta = #.###";theta
NEXT theta

Ao=(sumz-sumx)/(sumz+2*sumx)
PRINT USING "#.###";Ao

END
```

Figure 4. BASIC program for calculating the limiting fluorescence anisotropy  $A_0$ .

These integrals can be evaluated directly, yielding

$$\langle I_{||} \rangle = 1/5$$

and

$$\langle I_{\perp} \rangle = 1/15$$

Thus,

$$\langle I_{||} \rangle = 3\langle I_{\perp} \rangle$$

Hence

$$A_0 = 0.4$$

## Alternative Exercises in Numerical Calculation

The preceding result may be convincingly demonstrated by two alternative exercises in numerical calculation. Figure 4 gives a simple BASIC program that calculates the values of the two integrals (eqs 10 and 11) by systematic numerical summation, and hence the value of  $A_0$ .

The other procedure uses a Monte Carlo approach and is given in the BASIC program shown in Figure 5. This calculation has the didactic advantage of considering the random nature of molecular orientations. These cause the effective value of the quantity  $A_0$  to be an averaged one.

This program uses a random number generator to choose an orientation of the transition moment. Then the sums of the resolved components of the fluorescence emission are evaluated. Finally the emission anisotropy is calculated. When the program is run the value of the calculated fluorescence anisotropy soon converges and fluctuates around 0.39 to 0.41.

It is envisaged that this program could

- serve as the basis of a more elaborate program that could graphically display the random orientations of the transition moment and simultaneously carry out the calculation of  $A_0$
- be set as a computer programming assignment to enhance the student's understanding of fluorescence anisotropy
- be used to reinforce the result obtained upon the direct integration of eqs 10 and 11

# Physical Chemistry

```

p=3.14159
start:
REM: Randomize orientation of transition moment
theta=p*RND
phi=2*p*RND

REM: Calculate Iz=I(parallel) and Ix=I(perp.)
Iz=COS(theta)^4*SIN(theta)
Ix=COS(phi)^2*COS(theta)^2*SIN(theta)^3

sumz=sumz+Iz
sumx=sumx+Ix
Ao=(sumz-sumx)/(sumz+2*sumx)
PRINT USING "#.###";Ao
GOTO start

END

```

Figure 5. BASIC program that uses a Monte Carlo approach to calculate the limiting fluorescence anisotropy  $A_0$ .

## Literature Cited

1. Barltrop, J. A.; Coyle, J. D. *Excited States in Organic Chemistry*; John Wiley and Sons: London, 1975.
2. Perrin, F. J. *J. Phys.* **1926**, *7*, 390–401.
3. Perrin, F. J. *Phys. Radium* **1936**, *VII*, 7, 1–11.
4. Steiner, R. F.; McAlister, A. J. *J. Polym. Sci.* **1957**, *14*, 105–123.
5. Beddard, G. S.; Tran, C. D. *Eur. Biophys. J.* **1985**, *11*, 243–248.
6. Vandermeulen, D. L.; Jameson, D. M.; Thomas, V.; Vandermeer, B. W. *Biophys. J.* **1986**, *49*, 334–334.
7. Fujimoto, B. S.; Schurr, J. M. *J. Phys. Chem.* **1987**, *91*, 1947–1951.
8. Chang, M. C.; Flemming, G. R.; Yang, N. C. C.; Seanu, A. M. *Photochem. Photobiol.* **1988**, *47*, 345–355.
9. Fukumura, H.; Hayashi, K. J. *Coll. Interface Sci.* **1990**, *135*, 435–442.
10. Kettle, G. J.; Soutar, I. *Eur. Polym. J.* **1978**, *14*, 895–900.
11. Chiu, G.; Croucher, M. D.; Winnik, M. A. *Coll. Polym. Sci.* **1986**, *264*, 25–31.
12. Queslel, J. P.; Jarry, J. P.; Monnerie, L. *Polymer* **1986**, *27*, 1228–1234.
13. Sasaki, T.; Nishijima, Y.; Yamamoto, M. *Makromol. Chem. Rapid Comm.* **1986**, *7*, 345–350.
14. Ushiki, H.; Mita, I.; Tanaka, F. *Eur. Polym. J.* **1986**, *22*, 827–829.
15. Peterson, K. A.; Domingue, R. P.; Fayer, M. D.; Linse, S.; Zimmt, M. B. *Macromolecules* **1987**, *20*, 168–175.
16. Sasaki, T.; Nishijima, Y.; Yamamoto, M. *Macromolecules* **1988**, *21*, 610–616.
17. Fofana, M.; Veissier, V.; Viovy, J. L.; Monnerie, L. *Polymer* **1989**, *30*, 51–57.
18. Fuhrmann, J.; Hennecke, M. *Makromol. Chem., Macromol. Symp.* **1989**, *26*, 209–220.
19. Peterson, K. A.; Zimmt, M. B.; Jeng, Y. H.; Frank, C. W.; Fayer, M. D. *Macromolecules* **1989**, *22*, 874–879.
20. Sasaki, T.; Nishijima, Y.; Nawa, K.; Yamamoto, M. *Eur. Polym. J.* **1989**, *25*, 79–83.
21. Sasaki, T.; Yamamoto, M. *Macromolecules* **1989**, *22*, 4009–4013.
22. Cheng, K. H. *Chem. Phys. Lipids* **1989**, *51*, 137–145.
23. Van Langen, H.; Vanginkel, G.; Levine, Y. K. *Chem. Phys.* **1989**, *130*, 271–278.
24. Alder, M.; Tritton, T. R. *Biophys. J.* **1988**, *53*, 989–1005.
25. Bashford, C. L.; Morgan, C. G.; Radda, G. K. *Biochem. Biophys. Acta* **1976**, *426*, 157–172.
26. Nishijima, Y.; Teramoto, A.; Yamamoto, M.; Hiratsuka, S. *J. Polym. Sci., A2* **1967**, *5*, 23–35.
27. Beddard, G. S.; Allen, N. S. In *Comprehensive Polymer Science – Polymer Characterization*; Booth, C.; Price, C., Eds.; Pergamon: Oxford, 1989; Vol. 1, Chapter 22, p 499.
28. Mielenz, K. D.; Cehelnik, E. D.; McKenzie, R. L. *J. Chem. Phys.* **1976**, *64*, 370–374.
29. Jablonski, A. *Acta. Phys. Polon.* **1957**, *16*, 471–479. Chem. Abst. 52:7854d.
30. Bigger, S. W.; Ghiggino, K. P.; Meilak, G. A.; Verity, B. J. *Chem. Educ.* **1992**, *69*, 675–677.
31. Weltman, T. K.; Edelman, G. M. *Biochemistry* **1967**, *6*, 1437–1447.
32. Sawyer, W. H.; Dabscheck, R.; Knott, P. R.; Selinger, B. K.; Kuntz, I. D. *Biochem. J.* **1975**, *147*, 613–615.
33. Wahl, Ph. In *Time-Resolved Fluorescence in Biochemistry and Biology*; Cundall, R. B.; Dale, R. E., Eds.; NATO ASI Series A; Plenum: New York, 1983; Vol. 69, pp 497–521.
34. Ghiggino, K. P.; Tan, K. L. In *Polymer Photophysics*; Phillips, D., Ed.; Chapman and Hall: London, 1985; Chapter 7, p 351.
35. Witholt, B.; Brand, L. *Biochemistry* **1970**, *9*, 1948–1956.
36. Jonas, A.; Weber, G. *Biochemistry* **1971**, *10*, 1335–1339.
37. Stryer, L. *J. Mol. Biol.* **1965**, *13*, 482–495.
38. Weast, R. C., Ed. *CRC Handbook of Chemistry and Physics*; CRC Press: Boca Raton, U.S.A., 1990; p F-40.
39. McClure, R. J.; Craven, B. J. *Mol. Biol.* **1974**, *83*, 551–555.